Experimental study of $K_L^0 \to \pi^+\pi^-\gamma$ and other rare decay modes*

G. Donaldson,[†] D. Hitlin, R. Kennelly, J. Kirkby, J. Liu, A. Rothenberg,[‡] and S. Wojcicki

Physics Department and Stanford Linear Accelerator Center, Stanford University, Stanford, California 94305

(Received 15 July 1976)

Using the SLAC K_L^0 spectrometer facility, we have measured the ratio $(K_L^0 \to \pi^+\pi^-\gamma)/\Gamma(K_L^0 \to \text{all})$ to be $(6.2 \pm 2.1) \times 10^{-5}$. The ratio and Dalitz-plot distribution of 24 ± 10 events are consistent with CP conservation in this weak-electromagnetic decay. We have also set upper limits on various processes, as follows: $\Gamma(K_L^0 \to \mu^+\mu^-\gamma) / \Gamma(K_L^0 \to \text{all}) \le 7.8 \times 10^{-6}$, 90% C.L.; $\Gamma(K_L^0 \to \mu^+\mu^-\pi^0)/\Gamma(K_L^0 \to \text{all}) \le 5.7 \times 10^{-5}$, 90% C.L.; $\Gamma(K_L^0 \to \pi^+\pi^-e^+e^-) / \Gamma(K_L^0 \to \text{all}) \le 8.8 \times 10^{-6}$, 90% C.L.; $\Gamma(K_L^0 \to \pi^0\pi^\pm e^\mp\nu)/\Gamma(K_L^0 \to \text{all}) \le 2.2 \times 10^{-3}$, 90% C.L.

I. INTRODUCTION

A study of the rare decay modes of the K_L^0 meson spans a wide range of weak-interaction topics. Radiative decays of the neutral kaon potentially display the effects of weak neutral currents as well as possible CP noninvariance in the electromagnetic interactions of hadrons. In addition, a study of the kinematic behavior of the radiative processes may provide a test of various models of weak decays.

A run was made for a period equivalent to approximately 30 million K_L^0 decays, using the SLAC K_L^0 spectrometer facility, modified to detect photon- and electron-initiated showers. The apparatus also accepted the many decay channels having a π^0 in the final state, so that there was in principle a sensitivity to the decays $K_L^0 \to \pi^+\pi^-\pi^0$, $K_L^0 \to \pi^+\pi^-\gamma$, $K_L^0 \to \mu^+\mu^-\gamma$, $K_L^0 \to e^+e^-\gamma$, $K_L^0 \to \mu^+\mu^-\pi^0$, $K_L^0 \to e^+e^-\pi^0$, $K_L^0 \to \pi^\pm e^\mp\nu\gamma$, $K_L^0 \to \pi^+\pi^-e^+e^-$, $K_L^0 \to \pi^0\pi^\pm e^\mp\nu$, and $K_L^0 \to \pi^0\pi^+\pi^-\gamma$. This is quite an assortment, and it should be made clear at the outset that not only are some of these processes very rare indeed, but that the spectrometer is relatively ill adapted for certain of the decays mentioned above. The decay $K_L^0 \to \pi^+\pi^-\pi^0$ occurs with a branching ratio of order 10^{-1} and served as a normalization, whereas the next most likely decay is $K_L^0 \to \pi^\pm e^\mp\nu\gamma$, which is expected to occur with a branching ratio of order 10^{-3}. We have observed only the rare decay mode $K_L^0 \to \pi^+\pi^-\gamma$ and are thus left with the task of setting upper limits on the others. Each of these decays is predicted to occur at one level or another, and therefore a useful criterion for whether an upper limit is interesting or not is how it compares with the expected value for the branching ratio. In some cases, we are orders of magnitude from an interesting result, and correspondingly little effort has gone into refining the measurement.

Section II of this paper will describe the experimental procedures common to the entire experiment. Section III will deal with the decay K_L^0 $\to \pi^+\pi^-\gamma$ which is interesting for several reasons: the opportunity to observe another possible instance of CP violation, a potential testing ground for theoretical models of weak radiative decays, and the possibility that this decay could therefore interfere destructively as an intermediate state in the process $K_L^0 \to \mu^+\mu^-$. Section IV describes the decays $K_L^0 \to l\bar{l}\gamma$ (where l indicates e^- or μ^-), which occur either through the Dalitz pair process $K_L^0 \to \gamma\gamma$ followed by $\gamma \to l\bar{l}$, or through a direct process possibly involving neutral currents. The decay mode $K_L^0 \to l\bar{l}\pi^0$ will also be discussed in Sec. IV since it shares the neutral-current aspect of $K_L^0 \to l\bar{l}\gamma$. Section V will deal with the decay mode $K_L^0 \to \pi^+\pi^-e^+e^-$, while Sec. VI will focus on the process $K_L^0 \to \pi^0\pi^\pm e^\mp\nu$.

II. EXPERIMENTAL PROCEDURES

A. The SLAC K_L^0 spectrometer facility

The experiment was conducted at the SLAC K_L^0 spectrometer facility (Fig. 1), where we observed K_L^0 decays originating in a neutral beam which had a well-defined time structure. The decay products were detected by arrays of scintillation counters and wire spark chambers, positioned on both sides of a momentum-analyzing magnet. The counters served both to identify events of interest, and to provide timing information for the charged particles. Photons and electrons were identified by their characteristic showers following one of the thin lead converters, and muons by their penetration of the lead muon filter at the rear. Data were monitored by an on-line PDP-9 computer, and then transferred to magnetic tape for off-line analysis. This apparatus has been previously employed in several other experiments, and a complete description of the details of the beam, wire spark chambers, counter hodoscopes, and data acquisition logic may be found in Refs. 1–4.

One major modification made to the apparatus involved the rotation of the front hodoscope through
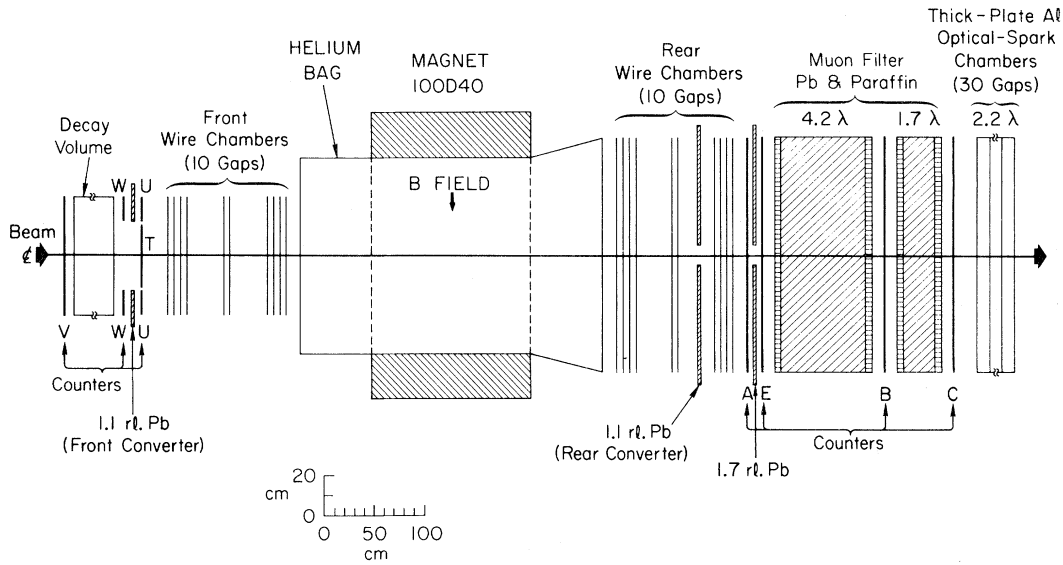
FIG. 1. Elevation view of the SLAC K_L^0 spectrometer. λ represents absorption lengths. Data from the E counters and optical spark chambers were not used in the analysis.

90° about its central axis, resulting in two columns of horizontal counters. In addition, various thin sheets of lead converters were strategically positioned, as shown in Fig. 1. The rear converter had a hole in its center to allow the passage of the neutral beam. A fraction of the wide-angle γ's converted in the lead between the W and the U bank, signaling their presence by a $\overline{W} \cdot U$. The more forward γ's traversed the magnet and converted in the rear lead converter, with the resulting showers triggering one or more A counters. Since a given photon or electron passed through only one lead converter, the conversion efficiency was limited to about 47% for γ's and 55% for electrons. We attempted to distinguish between electrons which did not convert in the rear lead converter and pions by means of a third 1.7 radiation length lead sheet inserted between the A and E counters. Electrons which showered would result in large pulse heights in the E bank. However, the correlation between leptonic events and high-E pulse height was not adequate, and we were thus unable to distinguish between pions and electrons which did not shower in the rear converter.

The logic signal for normal running was $\overline{V} \cdot 2T \cdot 2A \cdot (3A + \overline{W} \cdot U)$, where the two charged tracks following an incident neutral are indicated by $\overline{V} \cdot 2T \cdot 2A$, and the presence of a shower is inferred from either $\overline{W} \cdot U$ or $3A$.

Muons were identified by their ability to penetrate the muon filter and reach the B and C banks. The optical chambers following the C counters were intended to provide additional muon momentum in-

formation in the search for the muonic rare decay candidates. After the kinematical analysis, no events remained as candidates, and the information from the optical chambers was therefore not employed.

B. The data analysis

The data analysis was carried out in the following three major phases:

(1) reconstruction of track segments and location of conversion points of showers,

(2) matching of track segments through the magnet, and establishing the sign and momentum of each track,

(3) kinematic reconstruction to various hypotheses.

Only the method of shower location is described herein; a complete description of the other procedures may be found in Refs. 1–3.

The shower-finding software made use of the charged secondary's passage through the wire spark chambers (WSC). In the front chambers, shower elements emanating from the lead traversed the entire upbeam WSC system and were located as track segments. In the rear, they passed through only two X and two Y planes and were thus not normally reconstructed as tracks. A very intuitive approach was used to find the conversion points of the rear showers. X and Y lines were constructed through all pairs of sparks in the two X or Y chambers. A great many such lines were possible,

and to reduce the accidentals, we demanded that each line point to a counter that fired in the event, and that the slope of the line not exceed 45° relative to the beam axis. The line segments corresponding to shower candidates would then cluster at the plane of the rear lead converter. In general, even a good shower would have more than one cluster; however, these separate groupings would contain lines which shared common sparks. The best line for a shared spark was then chosen on the basis of the number of elements contributing to the corresponding cluster and the deviation of this line from the centroid of the cluster. After a cluster had been found, the contributing sparks were eliminated, and those remaining were again tested.

In general, a different number of clusters in X and Y could be found, and it remained to match a given X with its proper Y. In the front, this was done by using the association provided by the U and V sparks for the line segments. In the rear this information was not available for shower segments. However, since the A counters were equipped with a photomultiplier tube (PMT) at each end, the time difference between these two tubes was proportional to the vertical position of the track striking that counter, and allowed the independent X and Y clusters to be associated with the A counter that fired.

In the rear, electrons were identified by the presence of a track incident on the lead sheet followed by an emerging shower. Usually one outgoing element had the same direction as the incoming electron. However, various other categories of electron showers were observed, including showers which converged a short distance from the point at which a track passed through the lead. These were tentatively tagged as electrons when they converted within 5 cm of the track's projected intercept with the lead converter.

For a shower to be written onto output tape, the software had to locate at least one grouping in both X and Y which was consistent with the latch and timing information. If there was no corresponding incident track, the shower was passed as a photon. If a track pointed through the shower, then the track was identified as an electron and the shower was not passed.

The spatial resolution as shown in Fig. 2 was determined from electron showers. By examining the distance between the projected electron intersection and the shower conversion point, we found the shower resolution in the rear to be ±3.4 mm in both X and Y. Electrons were not identified for up-beam showers; however, a comparison of the shower conversion point with the projected intersection point of a track segment from the shower gave the resolution in front as ±1.25 cm in both projections.

C. Timing information

The time structure of the primary electron beam at SLAC enables a time-of-flight (TOF) measurement which serves to eliminate spurious triggers and provide consistency tests on the reconstructed kaon momentum.

In addition to spatial location of the shower conversion points, timing information was also available on the photon and electron showers. These differ from normal tracks in that several shower elements were present, and may impinge on more than one counter. If more than one element struck a particular A counter, the phototubes at each end recorded the arrival of the first available light, making the resulting time appear earlier by an amount proportional to the spread of the shower. This correction was taken into account in computing the time of the rear showers. γ-shower elements were also detected in the upstream U counters, which had only one PMT, requiring a correction for the transit time of flight along the counter. In both the front and the rear, multiple-counter showers were averaged. The event time was taken to be $t_{\text{meas}} = \frac{1}{2}[t_\gamma(\text{rear}) + t_\pm]$, where $t_\pm$ is the average of the two charged-track times. The time of the front showers was only used to check that the shower was associated with the charged tracks. Care was taken in correcting various effects as described above, such that the final systematic timing uncertainty was less than 0.1 nsec. This accuracy
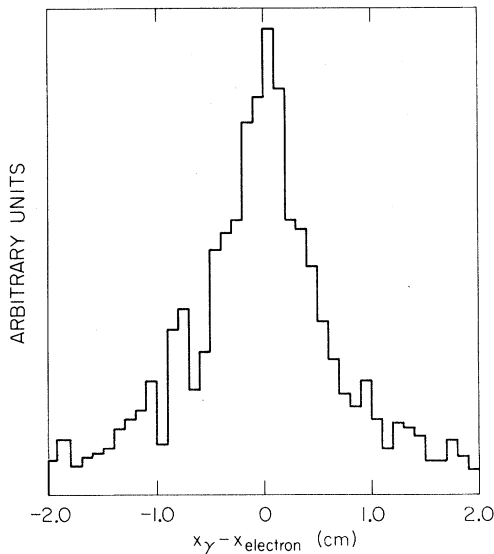

FIG. 2. Shower reconstruction resolution. x_{electron} is the projected intercept of an electron at the lead sheet; x_γ is the conversion point of the resulting shower.

enabled us to reject events wherein either the charged particle or the photon were significantly out of time relative to each other, as well as compare the measured time with that predicted from the kinematic reconstruction. The time resolution for the two charged tracks alone was 0.3 nsec; when the showers were included, it was reduced to 0.25 nsec. Figure 3 shows the various timing resolution curves.

D. The Monte Carlo simulation

In order to compute branching ratios we required a knowledge of the detection efficiency of the apparatus for the various decay modes. We studied the relevant efficiencies employing a Monte Carlo simulation of artificial events. In addition, this provided us with a basis of comparison whereby systematic effects in the spectrometer and background contaminations could be studied and eliminated. Such problems as the extraction of the momentum spectrum of the K_L^0 beam and the treatment of the wire chamber and timing data in the Monte Carlo simulation have been described in Ref. 5. It is worth repeating that many Monte Carlo simulations only record the relevant details of

FIG. 3. Timing resolution. (a) Front showers. (b) Rear showers. (c) Charged-track times. (d) Overall average $t_{meas} = \frac{1}{2}[t_\gamma \text{ (rear)} + t_\pm]$. $t_\pm$ is the average of the two charged-track times. t_{fit} is the actual event time determined kinematically.

events remaining at the final stage of the analysis. However, this shortcut does not allow a continuous comparison of simulated and real data at each stage of the reduction process. Accordingly, the output of our Monte Carlo simulation consisted of artificially generated raw data tapes with the same spark and counter format as written by the PDP-9. Subsequent analysis of these events paralleled the real data throughout the analysis.

One objective of the Monte Carlo simulation was to learn the conversion efficiency of photon and electron showers in the lead plates. The essential principle in the simulation of showers was to produce 100% conversion and detection efficiency, in order that the determination of the actual conversion probability in the data could be free of special effects dependent on techniques used in generating the shower. Shower losses in Monte Carlo data would then be limited to the geometric acceptance of the apparatus, and would not contain any of the complicated physics of shower propagation through the spectrometer. To this end, each simulated electron and photon incident on a lead sheet produced two electron-positron pairs leaving the lead sheet, thus guaranteeing that at least one shower element would traverse the chambers.
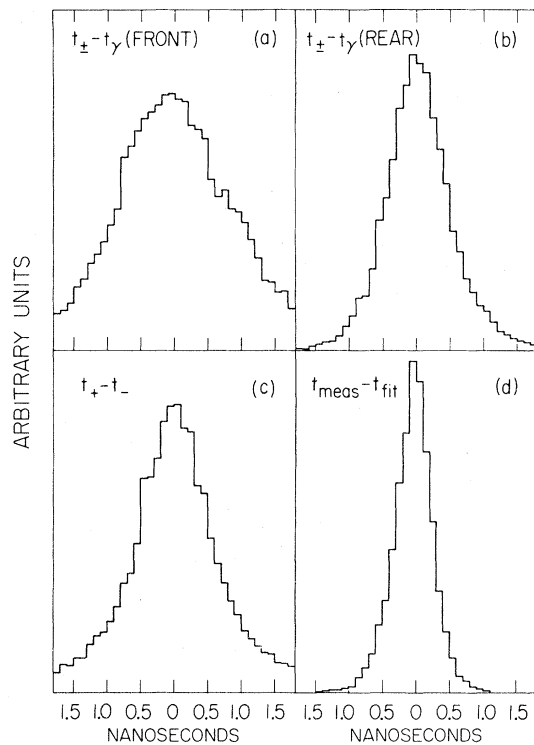
E. γ conversion efficiency

The determination of the conversion efficiency involved not only the intrinsic ability of a lead sheet to initiate a shower, but also the ability of the programs to recognize various configurations of sparks as a shower. In addition, functional dependences on position and energy must be correctly taken into account in order to use the correct shower conversion probability in determining the normalization and acceptances.

To obtain the global conversion probability, we isolated a sample of $K_{\pi 3}^0$ events in the data and compared the fractions of events in this sample containing one or two showers with the fractions observed in the Monte Carlo simulation at unit conversion efficiency. In general, this could be different for front and rear showers, although the converter thickness is the same in both cases. Three equations link the observed fractions with the unknown conversion efficiency:

$$N_2 = X^2 M_2 , \tag{1}$$

$$N_1 = X M_1 + 2X(1 - X)M_2$$
$$= X(M_1 + 2M_{2-}) - 2X^2 M_2 , \tag{2}$$

$$N_0 = M_0 + (1 - X)M_1 + (1 - X)^2 M_2$$
$$= (M_0 + M_1 + M_2) - X(M_1 + 2M_2) + X^2 M_2 , \tag{3}$$

where the variables are defined as follows: frac-

tion of events with 0, 1, or 2 γ's in the data $\equiv N_0, N_1, N_2$; fraction of events with 0, 1, or 2 γ's in the Monte Carlo simulation $\equiv M_0, M_1, M_2$; shower conversion and detection efficiency $\equiv X$, where X may be X_F or X_R for front or rear showers. Dividing (2) by (1) gives

$$X = \left(\frac{M_1}{M_2} + 2\right) \Big/ \left(\frac{N_1}{N_2} + 2\right). \tag{4}$$

We may not employ Eq. (3) in the normal data sample, since only inefficiencies in the trigger allowed the observed fraction N_0 to differ from zero.

A shower must satisfy certain quality requirements to be considered; in particular, the conversion point must lie within the boundary of the appropriate lead sheet (and not inside the hole through which the beam passed in the rear sheet), and its time information must be consistent with the time measured for the two charged tracks. Most γ's not associated with the decay which triggered the apparatus were removed by the condition that $\left| t_\gamma - t_\pm \right| < 1.0$ (2.0) nsec in the rear (front). However, certain accidental γ's fell within this time cut, and a correction was necessary to remove the contaminations they introduced into the observed fractions of real γ's.

Using Eq. (4), we find the conversion efficiencies to be $45.0 \pm 1.1\%$ in the front and $46.1 \pm 0.9\%$ in the rear. The accidental contaminations were calculated to be $0.3 \pm 0.1\%$ in the front and $2.6 \pm 0.3\%$ in the rear.

A subset of the data taken without a shower requirement (using a $2T \cdot 2A$ trigger) allowed us to use Eqs. (2) and (3) from which we obtain values for X_R of 45.0% and 46.4%, respectively, in excellent agreement with the previous result.

The underlying theory of photon-initiated showers is well understood, so that in principle one can calculate the probability of detecting a shower, given the incident energy and the thickness of the radiator. In practice, various approximations were necessary, such as those described by Rossi,[6] and from our measured γ spectrum, we estimate the conversion probability to be 55%. A direct experimental measurement has recently been published,[7] in which the maximum probability of detecting a charged particle after the thickness of the converter used in our experiment is measured to be 51 $\pm 3\%$. Having measured ~46%, we attribute the difference to TOF cuts eliminating real γ's and a small software inefficiency for locating showers in the data.

F. The momentum dependence of the γ conversion efficiency

The conversion efficiency is expected to be constant at high momentum; however, owing to the physical behavior of showers and certain software criteria, this efficiency must fall off for low-momentum γ's. To study this behavior, we selected only $K_{\pi 3}^0$ events which must also have two showers passing the quality requirements for the $\pi\pi\gamma$ analysis. As shown in Fig. 4, the intersection of a plane determined by the K_L^0 and the charged transverse momentum with the plane containing the two γ's specifies the direction of the π^0. The momentum of the π^0 is obtained by balancing the transverse momentum. Finally, the angles of the γ's with respect to the π^0 determine the momentum of each γ. The ratio $R = $ (number of γ's at p_γ in the data)/(number of γ's at p_γ in the Monte Carlo simulation) gives a number proportional to the conversion efficiency as a function of momentum. We conclude from Fig. 5 that for $p_\gamma \gtrsim 100$ MeV/c the conversion efficiency is constant. As one test of this method, we have generated Monte Carlo showers having a known conversion efficiency as a function of momentum. Using these showers as data, the shape of this function was accurately reproduced.

G. Normalization

The experimental problems associated with finding and reconstructing the decay modes $K_L^0 \to \pi\pi\gamma$ and $K_L^0 \to \pi\pi\pi^0$ are quite similar. Our primary measurement consists of the ratio R:

$$R = \frac{\Gamma(K_L^0 \to \pi^+\pi^-\gamma)}{\Gamma(K_L^0 \to \pi^+\pi^-\pi^0)}.$$

In this manner the uncertainties that were difficult to duplicate in the Monte Carlo simulation (such as the probability of finding showers and the TOF precision) tend to cancel, provided that both sets of data are treated similarly. In fact, since R is proportional to the probability of converting and detecting one γ from $\pi^+\pi^-\gamma$ decay, divided by the probability of converting and detecting either one or two γ's from the $\pi^+\pi^-\pi^0$ decay, the uncertainty in the branching ratio is insensitive to errors in the conversion efficiency.
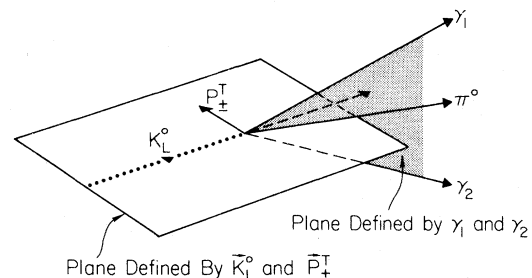

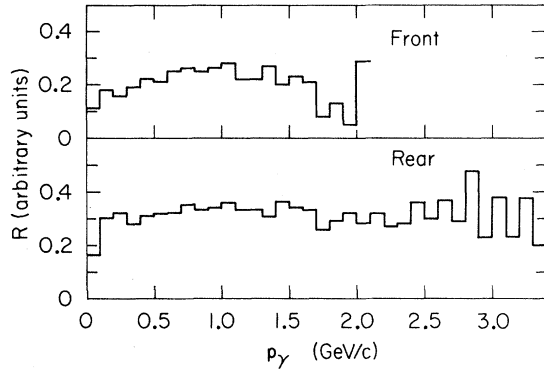FIG. 4. Reconstruction geometry for $K_L^0 \to \pi^+\pi^-\pi^0$ decays with the two γ's observed.

FIG. 5. Ratio R = (number of γ's at p_γ in data)/(number of γ's at p_γ in the Monte Carlo simulation).

We consistently required that events possess two charged tracks having a common vertex within the fiducial region, plus one or more showers. For purposes of normalization, we selected $K^0_{\pi 3}$ events by demanding the following:

(1) $-0.002 < p_0'^2 < 0.010$ (GeV/c)^2, where

$$p_0'^2 = \frac{(m_K^2 - m_{+-}^2 - m_{\pi 0}^2) - 4(m_{+-}^2 m_{\pi 0}^2 + m_K^2 p_T^2)}{4(p_T^2 + m_{+-}^2)},$$

in which m_{+-} represents the mass of the $(+-)$ system with both particles treated as pions, and p_T is its transverse momentum relative to the K^0_L axis,

(2) one or two γ's

(3) neither charged track be identified as an electron or a muon, and

(4) $\cos\theta_{\gamma C} < 0.9996$, where $\theta_{\gamma C}$ is the angle in the laboratory between the direction of the γ ray and either charged track at the decay vertex.

The final cut served to remove the K^0_{l3} background in which the γ is radiated by the lepton in passing through the front chambers or the hodoscope bank. Several other minor cuts were imposed: $p_{\pi 0}^T < p_{\pi 0}^*$, where $p_{\pi 0}^*$ is the π^0 c.m. momentum, $m_{\pi\pi} < m_K - m_{\pi 0}$, $|t_+ - t_-| < 1.5$ nsec, and $|t_{\gamma}-(t_+ + t_-)/2| < 1.0$ (2.0) nsec for rear (front) γ's.

Less than 1% of the 165K surviving events were due to leptonic contamination; however, losses because of pions which have simulated electrons or muons amounted to 10%. Of this, pion decays in flight were duplicated in the Monte Carlo simulation (approximately 4%) as well as showers from accidentally overlapping tracks causing an electron misidentification (a further 1–2%). Thus, roughly 5% of the 3π data was lost, introducing a small bias into the normalization. A negligible bias was also introduced by including low-momentum γ's for which the conversion efficiency was not determined. (Fewer than 1% have $p_\gamma < 150$ MeV/c.)

The acceptance was determined by comparing the number of Monte Carlo events which survived the above requirements with the number generated, making use of the proper γ conversion efficiency. We employed the recently determined[8] matrix element for $K^0_{\pi 3}$,

$$|M|^2 \sim 1 - 5.2(Q/M_K)Y + 4.64(Q^* M_K)^2 Y^2 ,$$

where

$$Y = 3T_{\pi 0}/Q - 1 ,$$

and the $K^0_{\pi 3}$ branching ratio

$$\Gamma(K^0_L \to \pi^+ \pi^- \pi^0)/\Gamma(K^0_L \to \text{all}) = 0.126 .$$

The number of kaons decaying was found to be 31.8 $\times 10^6$. Using completely reconstructed 3π events having two γ's, and making further kinematic requirements to eliminate completely the K^0_{l3} contamination provided a semi-independent verification which proved to be consistent with the ≥ 1 γ sample actually employed to ~10%.

III. THE DECAY $K^0_L \to \pi^+ \pi^- \gamma$

A. Theory

The decay $K^0_L \to \pi^+ \pi^- \gamma$ offers the following points of theoretical interest: a test of CP noninvariance in weak radiative decay, a comparison with several models, and a possible suppression of the $K^0_L \to \mu^+ \mu^-$ unitarity limit.

a. CP violation and the decay $K^0_L \to \pi^+ \pi^- \gamma$. It was pointed out some time ago that there is relatively little evidence that the electromagentic interactions of strongly interacting particles are invariant under C and T.[9] A radiative decay in the K system provides the logical testing ground in that K mesons display the only known violation of CP symmetry, and a radiative decay necessarily involves an electromagnetic interaction. The decays of this type with the highest branching ratio are the $K \to \pi\pi\gamma$ decays, and for this reason several experiments have used these decays to search for CP-violating effects. In the system of K mesons, various possibilities can exist for $K \to \pi\pi\gamma$: $K^\pm \to \pi^\pm \pi^0 \gamma$, $K^0_L \to \pi^+ \pi^- \gamma$, and $K^0_S \to \pi^+ \pi^- \gamma$. All of these decays can proceed through "inner bremsstrahlung" (IB), wherein the photon is radiated from one of the charged pions in the $K_{\pi 2}$ decay. Alternatively, it is possible, if the $K \to 2\pi$ decay proceeds through virtual intermediate states, that the photon may be emitted from one of the intermediate charged particles. This process is termed "direct emission" (DE) and is much less straightforward to calculate owing to the large number of possible intermediate states. In general, the rates for the direct processes depend on the specific constituents in the model for the decay, and are not necessarily related in any simple way. Experimental seaches

TABLE I. Quantum numbers of the final state for $K_L^0 \to \pi^+\pi^-\gamma$.

	$M1$	$E1$	$M2$	$E2$
$l_{\pi\pi}$	1	1	2	2
j_γ	1	1	2	2
$I_{\pi\pi}$	1	1	0,2	0,2
$C_{\pi\pi\gamma}$[a]	1	1	−1	−1
$P_{\pi\pi\gamma}$[b]	−1	+1	−1	+1
$CP_{\pi\pi\gamma}$	−1	+1	+1	−1

[a] $C = -(-1)^{l_{\pi\pi}}$.

[b] $P = \begin{cases} (-1)^{l_{\pi\pi}}(-1)^{j_\gamma+1} & \text{magnetic multipoles} \\ (-1)^{l_{\pi\pi}}(-1)^{j_\gamma} & \text{electric multipoles.} \end{cases}$

have been carried out for all of the above decays, and it is only recently that observation of any direct process has been reported.[10-12]

In the decay $K_L^0 \to \pi^+\pi^-\gamma$, CP nonconservation may be observed in several ways. First, there is a possible charge asymmetry in the momentum distribution of the π^+ and π^- which would arise from the interference of p and d waves of the $\pi\pi$ system.[13] However, even if CP violation were large in the matrix element, the expected result would attain only a maximum of a few percent since the $\pi\pi$ scattering phase shifts in the p and d waves are quite small. We observed only about 25 $\pi\pi\gamma$ events and were thus unable to check for such an asymmetry. Second, there is the possibility of observing interference between the decays $K_{L,S}^0 \to \pi\pi\gamma$.[14,15] Since only identical states can interfere, an inter-

ference would imply that the K_L^0 and K_S^0 are not pure CP eigenstates, which is of course already known from other experiments. Finally, both the expected rate and the energy distribution of the photon are sensitive to the CP nature of the final state.[16] The quantum numbers of various $\pi\pi\gamma$ states are shown in Table I. Note that the available energy of 215 MeV makes $L_{\pi\pi} > 2$ extremely unlikely, and $L_{\pi\pi} = 0$ is a forbidden "0 → 0" transition.

Since both the data from K_S^0 decays and $K^\pm$ decays favor the lowest-multipole emission, let us consider the energy distribution for $L_{\pi\pi} = 1$, CP (+ and −) states from the K_L^0. Inner bremsstrahlung ($E1, CP$ +) has a characteristic divergence at low-γ momentum, where as direct emission ($M1, CP$ −) peaks at $p_\gamma \approx 140$ MeV. In addition, the ratio

$$\Gamma(K_L^0 \to \pi^+\pi^-\gamma, \text{ IB})/\Gamma(K_L^0 \to \pi^+\pi^-) = 1.1 \times 10^{-2}$$

for $E_\gamma > 10$ MeV and 0.26×10^{-2} for $E_\gamma > 50$ MeV, corresponding to a total branching ratio 1.95×10^{-5} and 0.47×10^{-5}, respectively.[17] Thus we will compare both our measured rate and the energy distribution with the prediction for a CP-violating inner bremsstrahlung.

   b. *Calculations of the decay rate* $(K_L^0 \to \pi^+\pi^-\gamma)$. Theoretical efforts to calculate the rate for $K_L^0 \to \pi\pi\gamma$ were made over the past decade.[17-21] The earlier models primarily employed boson poles with various assumptions necessary to establish coupling constants. These are well described by Thatcher[22] and are summarized in Table II. In 1967, Lai and Young[17] used the method of current

TABLE II. Calculations for $R = \Gamma(K_L^0 \to \pi^+\pi^-\gamma)/\Gamma(K_L^0 \to \text{all})$.

	Date		Result
Theoretical results			
Chew, Ref. 18	1962	Boson-pole approximation	No quantitative result
Pepper and Ueda, Ref. 19	1964	Boson-pole approximation	6.7×10^{-4}
Oneda, Kim, and Korff, Ref. 20	1964	Boson-pole approximation	2.9×10^{-5}
Cline, Ref. 21	1965	$\Delta I = \tfrac{1}{2}$ rule	$\leqslant 2 \times 10^{-3}$
Lai and Young, Ref. 17	1967	Current algebra, PCAS	$(6.8 \pm 0.6) \times 10^{-5}$
		Inner bremsstrahlung	1.95×10^{-5}; $E > 10$ MeV
			0.47×10^{-5}; $E > 50$ MeV
Rockmore, Ref. 24	1970	Pion-pole model, Veneziano model	$9.14 \times 10^{-5} < R < 3.1 \times 10^{-4}$
Barshay, Ref. 25	1971	Hypothetical $\tilde{\rho}_0$ meson	1.04×10^{-5}
Moshe and Singer, Ref. 26	1972	Phenomenological Lagrangian, SU(3) breaking	$2.6 < R < 4 \times 10^{-4}$
Moshe and Singer, Ref. 27	1973	Details of constants adjusted	$(4.7^{+0.5}_{-0.2}) \times 10^{-4}$
Rockmore and Wong, Ref. 31	1973	Modified fermion-loop model	7.8×10^{-5}
Experimental results			
Anikina et al., Ref. 38	1966	Cloud chamber	< 0.02
Bellotti et al., Ref. 37	1966	Heavy-liquid bubble chamber	$< 5 \times 10^{-3}$
Nefkens et al., Ref. 36	1966	Spark chambers	$< 3 \times 10^{-3}$
Thatcher et al., Ref. 35	1968	Spark chambers	$< 4 \times 10^{-4}$
This experiment	1973	Wire spark chambers	$(6.2 \pm 1.9) \times 10^{-5}$

algebra and the partial conservation of axial-vector current (PCAC) hypothesis to calculate the ratio

$$\Gamma(K_L^0 \rightarrow \pi^+\pi^-\gamma, M1)/\Gamma(K_L^0 \rightarrow \gamma\gamma) = 0.14 .$$

The present branching ratio[23] for $K_L^0 \rightarrow \gamma\gamma = 4.9 \times 10^{-4}$ implies that $\Gamma(\pi\pi\gamma)/\Gamma(\text{all}) = 6.86 \times 10^{-5}$. Since that time, there have been several more attempts, including another pion-pole model by Rockmore in 1970,[24] and a model involving a hypothetical abnormal vector meson introduced by Barshay in 1971.[25] Neither of these gives a rate consistent with our measured branching ratio.

More recently, two other models for weak radiative decays have gained prominence. Moshe and Singer considered the possibility of a description of several weak radiative decays of K mesons, based on a phenomenological Lagrangian model which was fitted to the data from strong and radiative decays.[26] Their model has been applied to several K decays: $K_L^0 \rightarrow \gamma\gamma$, $K^+ \rightarrow e^+\nu\gamma$, $K^+ \rightarrow \pi^+\pi^0\gamma$, $K^+ \rightarrow \pi^+\gamma\gamma$, and $K_L^0 \rightarrow \pi^+\pi^-\gamma$ for which they predict

$$\Gamma(K_L^0 \rightarrow \pi^+\pi^-\gamma)/\Gamma(K_L^0 \rightarrow \text{all}) = 4.7^{+0.5}_{-0.2} \times 10^{-4} .\text{[27]}$$

As we shall see, this rate is roughly an order of magnitude above the measured value. This model involves certain SU_3-symmetry-breaking parameters described in detail by Singer.[28] Unfortunately for this approach, a certain combination of these parameters depends on the decay rate for $\eta \rightarrow 2\gamma$, and a new measurement[29] of $\Gamma(\eta \rightarrow \gamma\gamma)$ implies that the MS model no longer gives satisfactory agreement with the experimental value for $\Gamma(K_L^0 \rightarrow \gamma\gamma)$ which is fundamental to their calculation of $\Gamma(K_L^0 \rightarrow \pi\pi\gamma)$. These developments are rather recent, and it remains to be seen whether they can be incorporated into the model in a consistent manner.

The other recent approach to the radiative decays of K mesons is an extension of Steinberger's baryon-loop model[30] originally proposed to calculate the π^0 lifetime. Rockmore and Wong[31] applied this technique to a calculation of $K_L^0 \rightarrow \gamma\gamma$ and obtained

$$\Gamma(K_L^0 \rightarrow \gamma\gamma)/\Gamma(K_L^0 \rightarrow \text{all}) = 1.35 \times 10^{-4} ,$$

compared with the experimental value of 4.9×10^{-4}. This agreement is quite surprising considering that the calculation involved no free parameters, and that the agreement is no worse than in the case of the π^0. They then proceeded to calculate the rates for $K^+ \rightarrow \pi^+\pi^0\gamma$ and $K^+ \rightarrow \pi^+\gamma\gamma$. In the case of the decay $K_L^0 \rightarrow \pi\pi\gamma$, the calculation[32] yields directly the value

$$\Gamma(K_L^0 \rightarrow \pi^+\pi^-\gamma)/\Gamma(K_L^0 \rightarrow \text{all}) = 7.5 \times 10^{-5} .$$

c. The decay $K_L^0 \rightarrow \pi^+\pi^-\gamma$ and the $K_L^0 \rightarrow \mu^+\mu^-$ puzzle. Historically, the controversy over an experimental result[33] for $K_L^0 \rightarrow \mu^+\mu^-$ spurred a great deal of activity, not only to search for weak neutral

currents, but to understand why this decay appeared to contradict a fundamental lower limit for its rate.[34] One theoretical conjecture was that the decay $K_L^0 \rightarrow \pi\pi\gamma$ may interfere with the $\pi\pi$ amplitude via the process shown in Fig. 6.

Based on the previous experimental limit,[35-38]

$$R = \Gamma(K_L^0 \rightarrow \pi^+\pi^-\gamma)/\Gamma(K_L^0 \rightarrow \text{all}) < 4 \times 10^{-4} ,$$

it was originally proposed that the suppression to the $K_L^0 \rightarrow \mu^+\mu^-$ rate could reach 20%.[39] However, subsequent calculations reduced this estimate to ~4%. The most detailed of these is by Alles, Gaillard, and Pati,[40] who find that the suppression depends on a factor $[\Gamma(K_L^0 \rightarrow \pi\pi\gamma)/\Gamma(K_L^0 \rightarrow \gamma\gamma)]^{1/2}$, and that possible reductions due to other intermediate states are negligible.

B. Kinematical analysis

The extraction of the $\pi\pi\gamma$ signal involved the isolation of a maximum of several hundred events (at the previous upper limit for the rate) from a sample containing hundreds of thousands of candidates. This selection was aided by our knowledge of the γ direction which provided a two-constraint fit, without relying directly on the TOF for the kaon momentum.

Candidates for $\pi\pi\gamma$ decay were selected using kinematic cuts similar to those used for the 3π normalization sample:

(1) $p_0'^2 < -0.014$ to eliminate the bulk of the $K_{\tau 3}^0$ triggers,

(2) one and only one γ,

(3) neither charged track identified as an electron or muon, and

(4) $\cos\theta_{\gamma C} < 0.9996$ to eliminate leptonics with bremsstrahlung. Several other minor kinematical cuts were made: (a) $m_{\pi\pi} < m_K$, (b) $p_\gamma^T < p_\gamma^*$, where p_γ^* is the c.m. momentum of the γ, (c) a timing consistency check on the charged tracks and γ: $|t_+ - t_-| < 1.5$ nsec and $t_\gamma - |\frac{1}{2}(t_+ + t_-)| < 1.0$ (2.0) for a rear (front) γ. The remaining background is primarily $K_{\tau 3}^0$ (negative $p_0'^2$) having a random γ in
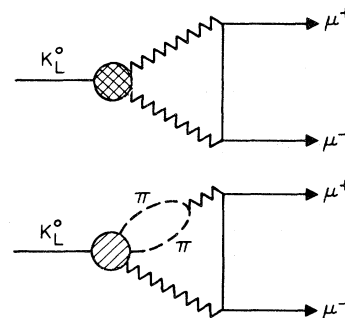

FIG. 6. Processes contributing to $K_L^0 \rightarrow \mu^+\mu^-$.

time with the charged tracks. The contribution from $K_{\pi 3}^0$ is quite small, having been eliminated by the $p_0'^2$ cut. The magnitudes and distributions of these are discussed below.

Two methods were used to identify $\pi\pi\gamma$ events: The first compared the predicted direction of the γ ray with its measured direction, and the second compared $m_{\pi\pi\gamma}$ to m_K. At the outset, we calculated the γ momentum by balancing transverse momentum and rejected events with $p_\gamma < 150$ MeV/c, since we had no accurate knowledge of the conversion efficiency below this energy. In the first method, we calculated ψ, the angle between the measured and predicted γ-ray direction using $\vec{p}_{\pi^+}$, $\vec{p}_{\pi^-}$, and the K_L^0 direction as shown in Fig. 7. There are two solutions for the laboratory γ direction because of the quadratic ambiguity corresponding to forward and backward emission in the K_L^0 center-of-mass system. The solution which gives the better agreement with the measured direction was chosen, thereby specifying an associated kaon momentum. The TOF (τ) associated with the kaon momentum was then compared to the measured time, and we demanded that

$$|\tau_{\text{meas}} - \tau_{\text{fit}}| \leq 0.7 \text{ nsec} .$$

Although the resolution in $\cos\psi$ was well behaved as $\theta_{\gamma K} \to 0$, the slight enhancement at $\theta_{\gamma K} = 0$ observed in the background imposed a requirement that $\theta_{\gamma K}^2 > 0.001$. After this cut, 106 front-shower and 786 rear-shower events remained, and their values for $\cos\psi$ are shown in Figs. 8(a) and 8(b). Note that if our expectation that the background came predominantly from random γ's is correct, then the background should be flat in $\cos\psi$. For example, if the γ was predicted to hit a given point on the lead sheet, and the randoms were uniformly distributed in this plane, then the number dN of randoms between r and $r + dr$ would be approximately $2\pi\overline{Z}^2\sin\psi d\psi$, where $\overline{Z}$ is the average flight path of the γ ray and ψ is its angle with respect to the Z
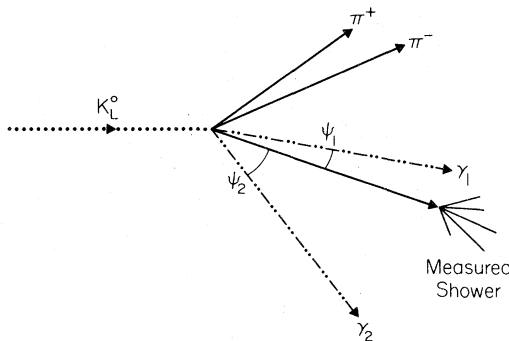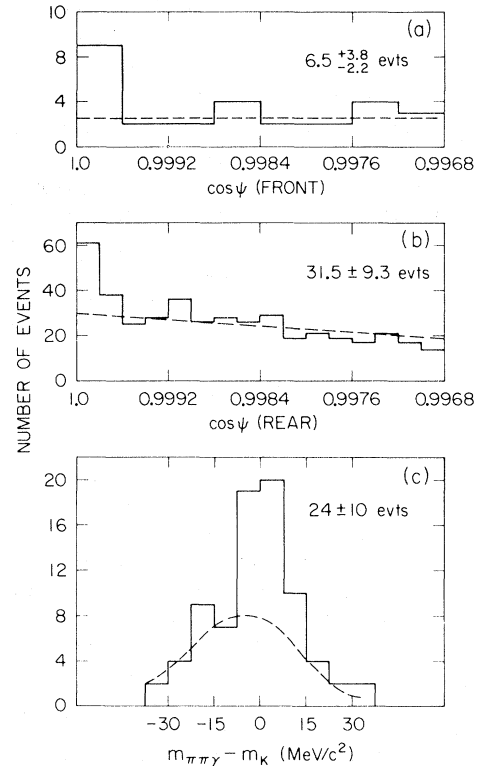

FIG. 8. (a) $\cos\psi$, the angle between the measured and predicted γ-ray directions for $\pi\pi\gamma$ candidates with a front γ shower. (b) $\cos\psi$ for $\pi\pi\gamma$ candidates with a rear γ shower. (c) $m_{\pi\pi\gamma} - m_{K^0}$. The backgrounds discussed in the text are indicated by dashed lines.

axis. Thus $dN/d(\cos\psi) \propto 2\pi\overline{Z}^2$, resulting in a flat background in $\cos\psi$.

The second method consisted of reconstructing the mass of the $\pi\pi\gamma$ system. First, the candidates were required to be balanced in transverse momentum by applying $\Delta\phi$ cuts of 450 (150) mrad for the front (rear) showers, where $\Delta\phi$ is the difference between the predicted and measured γ angle in the plane perpendicular to the K_L^0 direction.
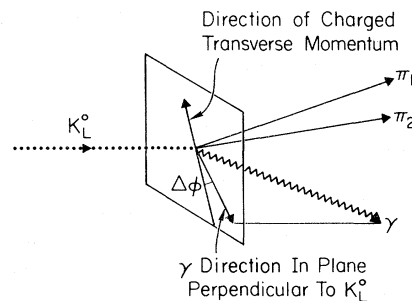

FIG. 7. Reconstruction geometry for $\cos\psi$ in $K_L^0 \to \pi^+\pi^-$ decay.

FIG. 9. Reconstruction geometry for $m_{\pi\pi\gamma}$ in the $K_L^0 \to \pi^+\pi^-\gamma$ decay.

Figure 9 shows the geometry for this reconstruction.

The γ momentum was then computed using the measured transverse momentum and the γ direction: $|p_\gamma| = |p_\perp|/\sin\theta_{\gamma K}$. A fitted TOF corresponding to the momentum of the kaon as computed from all the outgoing particles was then compared to the measured momentum, and again we required that

$$|\tau_{\text{fit}} - \tau_{\text{meas}}| < 0.7 \text{ nsec}.$$

The $\Delta\phi$ cut reduced the 1074 candidates to 79, whose invariant mass is plotted in Fig. 8(c), where

$$M_{\pi\pi\gamma}^{2} = M_{\pi\pi}^{2} + 2p_{\pi\pi}^{2}\left(\frac{\sin\theta_{\pm K}}{\sin\theta_{\gamma K}}\right)\left[\left(1+\frac{M_{\pi\pi}^{2}}{p_{\pi\pi}^{2}}\right)^{1/2} - \cos\theta_{\pm\gamma}\right]$$

$$\simeq M_{\pi\pi}^{2} + \frac{p_{\pi\pi}^{2}\theta_{\gamma}^{2}\theta_{\pm K}}{\theta_{\gamma K}},$$

where $M_{\pi\pi} \equiv$ invariant mass of dipion system, $p_{\pi\pi}$ $\equiv$ magnitude of dipion momentum, $\theta_{\pm K} \equiv$ angle between $\pi^+\pi^-$ system and kaon, $\theta_{\pm\gamma} \equiv$ angle between the $\pi^+\pi^-$ system and the γ, and $\theta_{\gamma K} \equiv$ angle between the γ and the kaon. Note that the mass of the $\pi\pi\gamma$ system is not well defined as $\theta_{\gamma K}$ goes to zero. Therefore, as in the "$\cos\psi$ method," we imposed the requirement that $\theta_{\gamma K}^{2} > 0.001$ or that $\theta_{\gamma K} > 33$ mrad.

We conclude from Figure 8 that both methods yield significant evidence for the presence of a $\pi\pi\gamma$ signal. However, we must still investigate whether any of the potential sources of background could have peaked at $m_{\pi\pi\gamma} = m_K$ or at $\cos\psi = 1.0$. For this purpose, we note that different regions of $p_0'^2$ imply different sources of background, as shown in Fig. 10.

The decay $K_L^0 \to \pi^+\pi^-\pi^0$ would be expected to be the prime source of any background since there are two pions and two γ's in the final state, of which we may have detected only one. However, $p_0'^2 > 0$ is an extremely effective cut for the decay, and we can check that no enhancement at $p_0'^2$ ~ -0.014 still persists after cuts. In addition, we estimated the detailed shape of the $p_0'^2$ distribution for $K_{\mp3}^0$ in the negative $p_0'^2$ region by selecting events on the data-summary tape (DST) having two γ's, but which passed all the $\pi\pi\gamma$ cuts except for $p_0'^2$ and the closely related p_γ^T cut. After making a correction for leptonic feedthrough into the $K_{\mp3}^0$ sample via random γ's, we calculated the fraction of $K_{\mp3}^0$ within the $\pi\pi\gamma$ region which appeared as candidates in the "$\cos\psi$" method. Knowledge of this fraction and the total number of $K_{\mp3}^0$ decays enabled us to calculate the number of such background events contaminating the $\cos\psi$ plot. We find this contamination to be less than 5% (or <50 events). Furthermore, Monte Carlo simulations of $K_{\mp3}^0$ decays showed no evidence of peaking in the signal region, even if pathologically large scatters were
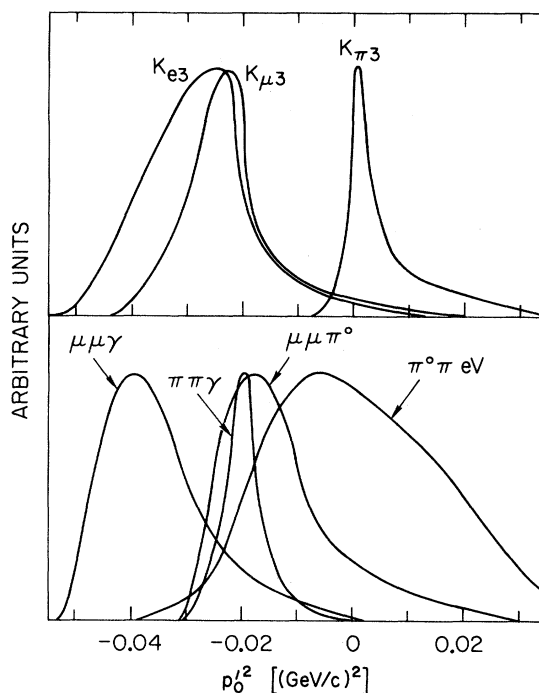

FIG. 10. Distributions of $p_0'^2$ for various K_L^0 decays.

introduced into kaon or pion directions. This source of background also could not account for the observed peak in the mass plot, since the additional 10^{-2} reduction due to the $\Delta\phi$ requirement left too few potential $K_{\mp3}^0$'s on the mass plot, and these events showed no peak at $m_{\pi\pi\gamma} = m_K$.

The decay $K_L^0 \to \pi^\pm$ ($\mu^\mp$ or $e^\mp$, unidentified) ν plus an accidental in-time shower could also contribute to the $\pi\pi\gamma$ signal, since $p_0'^2$ for this decay overlaps the $\pi\pi\gamma$ region. We simulated this decay using Monte Carlo K_{l3}^0 events together with a "random" γ. We also selected events on the DST in which the lepton was identified and compared their distributions with those in the final data sample. Finally, we assumed that all the events on the $\cos\psi$ plot were K_{l3}^0 with a random γ except for the true signal. These were then studied by reshuffling the γ's so that the photon (which had already passed all the timing and quality requirements) was reassigned to another event. To the extent that the signal events constituted a small fraction of the candidates, this technique had a built-in normalization, as well as the assurance that the photons had as many real characteristics as possible. All of these techniques share the common result that in no case was a peak observed in the signal region, so that even though these events form the bulk of the DST, they could not have accounted for the signal we observed. The process of reassigning γ's to another event reproduced the shape of the distribution outside the sig-

nal so well that we generated several such reshuf-flings to obtain a smooth fit to the random γ back-ground.

The dashed lines on Fig. 8 represent the averaged results of the contributions from background. We note that the background subtraction does not de-pend strongly on which method we use; at this level, an eyeball fit or a fit to the tails of the dis-tribution would serve adequately. However, we choose to employ the random-γ technique since it was well understood and appeared to explain the background the best.

The three distributions of Fig. 8, when combined with the Monte Carlo acceptance calculations (for which the matrix elements are discussed in the fol-lowing section) and the $K_{\pi 3}^0$ normalization, provide three correlated determinations of the $K_L^0 \to \pi\pi\gamma$ branching ratio. In all cases, we increased the systematic uncertainty on the background since we have not included explicit subtractions for $K_{\pi 3}^0$ or $K_{l3+\gamma}^0$. For the "mass" method, we accepted events within ± 7.5 MeV of m_K, from which we obtained $(39 - 15) \pm 6.2$ (statisitical uncertainty) ± 8 (back-ground uncertainty) $= 24 \pm 10$ events. For the "$\cos\psi$" method, we accepted events with $\cos\psi_F > 0.9996$, from which we obtained $(9 - 2.5) \pm 3.7$ (statistical) ± 1 (background) $= 6.5_{-2.2}^{+3.8}$ events, and for $\cos\psi_R$ > 0.9998 we had $(61 - 29.5) \pm 7.8$ (statistical) ± 5 (background) $= 31.5 \pm 9.3$ events. These then yield $R \equiv \Gamma(K_L^0 \to \pi^+\pi^-\gamma)/\Gamma(K_L^0 \to \pi^+\pi^-\pi^0)$:

Mass plot: $R = (3.9 \pm 1.6) \times 10^{-4}$,

$\cos\psi_F$: $R = (5.3 \pm_{1.8}^{3.1}) \times 10^{-4}$,

$\cos\psi_R$: $R = (5.8 \pm 1.6) \times 10^{-4}$.

Weighting these results and uncertainties by $1/\sigma^2$ gives an overall average value of

$R = (4.9 \pm 1.7) \times 10^{-4}$.

Using $\Gamma(K_L^0 \to \pi^+\pi^-\pi^0)/\Gamma(K_L^0 \to \text{all}) = 0.126$, this cor-responds to

$\Gamma(K_L^0 \to \pi^+\pi^-\gamma)/\Gamma(K_L^0 \to \text{all}) = (6.2 \pm 2.1) \times 10^{-5}$.

C. Dalitz-plot distribution for $K_L^0 \to \pi\pi\gamma$

As mentioned in the discussion of the theoretical aspects of $K_L^0 \to \pi\pi\gamma$, the decay can proceed either through the CP-violating $K_L^0 \to \pi^+\pi^-$ + a photon from inner bremsstrahlung (IB), or via a CP-conserving direct emission (DE) process. Since the brems-strahlung process should populate the low-γ-mo-mentum region in the center of mass, it would be easily distinguishable from the direct process which tends to maximize the γ momentum.

In Fig. 11, we show the Dalitz plot, folded about the γ energy axis, for those events lying within ± 7.5 MeV of m_K in Fig. 8(c). These events had a
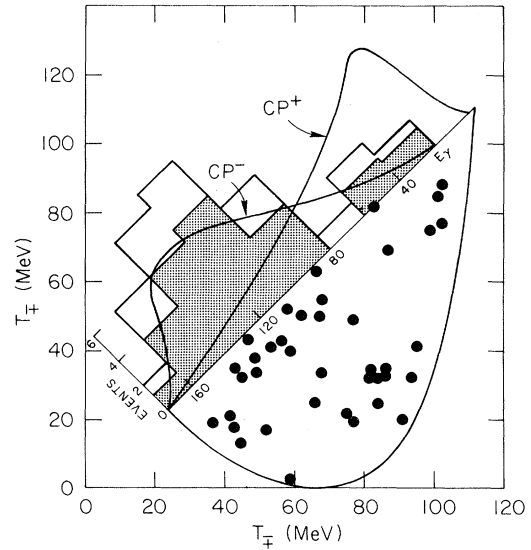

FIG. 11. Dalitz plot (folded about the γ energy axis) and projected γ-ray energy spectrum. The shaded por-tion is the difference between the observed distribution and the expected background. The smooth curves show the predicted spectra including experimental acceptance for $L_{\pi\pi} = 1$, CP-conserving (−) and CP-violating (+) ma trix elements.

signal-to-noise ratio of roughly $3:2$. The γ energy spectrum for the signal as well as the expected background are also shown in Fig. 11.

Since it appears most likely that the emission is $E1$ or $M1$ (the lowest possible angular momentum state), we generated both these possibilities using the matrix elements as given by Beder.[16] The re-sulting γ spectra with the experimental acceptance included are shown in Fig. 11. Qualitatively, the $L_{\pi\pi} = 1, CP -$ matrix element due to magnetic dipole emission resembles a phase-space distribution. The bremsstrahlung $[L_{\pi\pi} = 1, CP +]$ distribution peaks distinctively at low p_γ, with the cutoff due to the requirements that $p_\gamma > 150$ MeV in the lab system. Our data favor the $M1$ matrix element.

D. Conclusions

The measured branching ratio is consistent with only two of the calculations previously discussed. These are the 1967 current-algebra calculation of Lai and Young,[17] and the zero-free-parameter baryon-loop model of Rockmore and Wong[32] in 1973.

Lai and Young predict

$\Gamma(K_L^0 \to \pi\pi\gamma , \text{DE})/\Gamma(K_L^0 \to 2\gamma) \simeq 0.14$;

therefore, when the present value

$\Gamma(K_L^0 \to 2\gamma)/\Gamma(K_L^0 \to \text{all}) = 4.9 \times 10^{-4}$

is used, we expect that

$$\Gamma(K_L^0 \to \pi\pi\gamma)/\Gamma(K_L^0 \to \text{all}) \simeq 6.8 \times 10^{-5} \ .$$

Rockmore and Wong approach the problem via a modified fermion-loop model which has no adjustable parameters. Their unrenormalized result is $R = 7.51 \times 10^{-5}$, which is in good agreement with our measurement.

If the decay proceeds via the CP-violating mode $K_L^0 \to \pi\pi$ followed by inner bremsstrahlung, one expects a branching ratio of roughly 1×10^{-5} (for $E_\gamma^* > 20$ MeV) as well as the bremsstrahlung energy distribution. From the crude Dalitz-plot distribution of the observed $\pi\pi\gamma$ and the measured branching ratio, the data are consistent with a CP-conserving magnetic dipole transition dominating the decay.

Finally, Alles, Gaillard, and Pati estimate[40] that the maximum suppression to the $K_L^0 \to \mu\mu$ rate due to the $\pi\pi\gamma$ intermediate state is 2–4 % using the previous upper limit on $K_L^0 \to \pi\pi\gamma$. Their expression for the suppression includes a factor $[\Gamma(K_L^0 \to \pi\pi\gamma)/\Gamma(K_L^0 \to 2\gamma)]^{1/2}$, which when modified using current values implies that the maximum decrease in the $K_L^0 \to \mu^+\mu^-$ unitarity limit is 1.6%.

IV. THE DECAYS $K_L^0 \to l\bar{l}\pi^0$

A. Theory

Weak decays of the K_L^0 in which two leptons with zero total charge occur in the final state can proceed via a strangeness-changing neutral current. This current is excluded to a high sensitivity by

the measured $K_L^0 \to \mu^+\mu^-$ branching ratio.[34] It is of interest to confirm further this result be measuring the rates for $K_L^0 \to \mu^+\mu^-\gamma$ and $K_L^0 \to \mu^+\mu^-\pi^0$ and comparing the branching ratios with those expected from "conventional" mechanisms.

The calculation of the Dalitz-pair rate $\Gamma(K_L^0 \to l\bar{l}\gamma)/\Gamma(K_L^0 \to \gamma\gamma)$ is relatively straightforward, and yields a ratio of 1.6×10^{-2} for electrons and 4.1×10^{-4} for muons.[41] This decay may exhibit structure effects due to a form factor parametrized by the lepton-pair mass,[42] which would modify the expected branching ratios slightly (see Table III) and would appear as a small distortion in the lepton-pair mass spectrum. The $K_L^0 \to l\bar{l}\gamma$ decay could also proceed through some sort of neutral-current mechanism. One such possibility has been considered using a Hamiltonian proposed by Wolfenstein, wherein the original goal was to suppress the decay $K_L^0 \to \mu\bar{\mu}$ by allowing a destructively interfering, CP-violating transition $K_S^0 \to \mu\bar{\mu}$. Using this Hamiltonian, Singh has calculated[43] a branching ratio for the decay $K_L^0 \to \mu\bar{\mu}\gamma$, for which he obtains 3.4×10^{-7}, or roughly twice the Dalitz-pair rate. Finally, a model proposed by Alles and Pati[44] involving a hitherto undetected light neutral boson decaying to μ pairs would predict a very large rate for $K_L^0 \to \mu\mu\gamma$, on the order of 6×10^{-4}.

A measurement of the decay $K_L^0 \to l\bar{l}\pi^0$ could serve as a test of several theoretical ideas[45,46]: The decay could proceed as a second-order weak process, or alternatively could arise as an electromagnetic effect superimposed on a lowest-order

TABLE III. Calculations for $R = \Gamma(K_L^0 \to \text{rare mode})/\Gamma(K_L^0 \to \text{all})$.

Decay	Theorist		Result
$K_L^0 \to l\bar{l}\gamma$	Miyazaki, Ref. 41	Dalitz pairs and $K_L \to \gamma\gamma$ rate	8.3×10^{-6} for $ee\gamma$
			2.1×10^{-7} for $\mu\mu\gamma$
	Singh, Ref. 43	CP-odd nonelectromagnetic interactions,	$(2.2-5.2) \times 10^{-7}$ for $ee\gamma$
		"Wolfenstein Hamiltonian"	$(1.5-3.4) \times 10^{-7}$ for $\mu\mu\gamma$
	Alles and Pati, Ref. 44	Light neutral boson decaying to $\mu^+\mu^-$	$> 6 \times 10^{-4}$ for $\mu\mu\gamma$
	Sehgal, Ref. 42	Various structure effects in matrix	$(7.8-8.1) \times 10^{-6}$ for $ee\gamma$
		element	$(2.0-2.7) \times 10^{-7}$ for $\mu\mu\gamma$
		Experimental upper limit	$(<2.8 \times 10^{-5})$ for $ee\gamma$
		No experimental upper limit for $\mu\mu\gamma$	
$K_L^0 \to l\bar{l}\pi$	Okubo and Bace, Ref. 47	Strong internal coupling intermediate	$\lesssim 1.65 \times 10^{-6}$ for $ee\pi$
		vector bosons (IVB)	$\lesssim 0.65 \times 10^{-6}$ for $\mu\mu\pi$
	Pais and Trieman, Ref. 45	Order-of-magnitude estimate,	$\sim 10^{-6}$
		no experimental upper limit	
$K_L^0 \to \pi^0\pi e\nu$	Weinberg, Ref. 60	Current algebra and PCAC	5×10^{-5}
	Bace and Okubo, Ref. 59	IVB model	1.23×10^{-4}
	Behrends, Donnachie, and Oades, Ref. 58	Fit to $K^\pm$ data, no experimental upper limit	$0.79-1.2 \times 10^{-4}$
$K_L^0 \to \pi^+\pi^-e^+e^-$	Majumdar and Smith, Ref. 53	Vector-meson dominance, current algebra, $K_L \to \gamma\gamma$ rate	1.7×10^{-7}
	Okubo and Bace, Ref. 47	IVB model	3.4×10^{-9}
	Anikina *et al.*, Ref. 49	Experimental upper limit	$< 3.0 \times 10^{-5}$

nonleptonic interaction. In other models, more complicated couplings are present, and if sufficient data could be acquired it might become possible to determine whether or not there is a nonlocal lepton coupling. Further speculation is the possibility of observing the decay of heavy leptons via the process $K \to L\bar{l}$ followed by $L \to \pi l$. Reliable calculations for higher-order weak interactions are very difficult, and only one estimate for $K_L \to l\bar{l}\pi^0$ appears in the literature. This arises in the model of Okubo and Bace,[47] who consider a group of intermediate vector bosons which have strong interactions among themselves but are coupled weakly (or electromagnetically) to all other particles. This model is directed to the decay modes $K_{L,S}^0 \to \mu^+\mu^-$; however, it also allows a calculation of the rates for $K_L^0 \to l\bar{l}\pi^0$, $\pi^+\pi^-e^+e^-$, and $\pi^0\pi^\pm e^\mp\nu$ (see Table III).

B. Kinematic analysis

The observation of two muons penetrating the lead wall provides a signature which is not easily duplicated by background processes. The additional presence of one or more valid photon showers then implies an extremely pure sample in which to test the hypothesis $K_L^0 \to \mu^+\mu^-\gamma$ or $\mu^+\mu^-\pi^0$. The spectrometer was well adapted to resolve these events, making use of the two-stage muon filter and the excellent shower conversion point resolution. However, the expected rates are very low ($\sim 10^{-7}$) and the geometric acceptance is small. Thus it is not surprising that, in some $3 \times 10^7 \, K_L^0$ decays, we have observed no events.

To begin the reconstruction, we selected those events containing two identified muons which have a vertex and one or more photon showers. One shower is sufficient to overdetermine the decay $K_L^0 \to \mu^+\mu^-\gamma$; however, two are required for the decay $K_L^0 \to \mu^+\mu^-\pi^0$. The necessity of detecting both photons from the π^0 decay reduces the sensitivity for $\mu\mu\pi^0$ by roughly an order of magnitude relative to the $\pi\pi\gamma$ decay.

a. $K_L^0 \to \mu\mu\gamma$. Events having only one shower were tested as $\mu\mu\gamma$ candidates. The following two minor kinematical requirements were imposed:

(1) $m_{\mu\mu} < m_K$, where $m_{\mu\mu}$ is the invariant mass of the 2μ system,

(2) $p_\gamma^T < p_\gamma^*$, where p_γ^T is the transverse momentum of the γ ray, p_γ^* is the momentum of the γ in the kaon rest frame.

The event topology was then required to have transverse momentum balance, and the direction of the γ was required to be opposite the charged transverse momentum. We required $\Delta\phi$ to be less than 450 (150) mrad for front (rear) showers, where $\Delta\phi$ is the difference between the predicted

and measured γ angle in the plane perpendicular to the K_L^0 direction. (Since we wound up with no viable candidates, it was not necessary to impose cuts on p_γ or $\theta_{\gamma K}$ as it was in the $\pi\pi\gamma$ analysis.) The above cuts reduced the 383 candidates to 43 [see Fig. 12(a)].

We reconstructed the mass of the $\mu\mu\gamma$ system exactly as for $\pi\pi\gamma$, using p_{μ^+}, p_{μ^-}, and $p_\gamma = p_\pm^T/\sin\theta_{\gamma K}$, where $p_\pm^T$ is the sum of the charged transverse momentum and $\theta_{\gamma K}$ is the angle between the photon and the kaon. We expect the following two sources of background:

(a) $K_{\pi 3}^0$ decays (having positive $p_0'^2$) in which both pions have decays or penetrated the Pb wall,

(b) $K_{\mu 3}^0$ decays (negative $p_0'^2$) followed by π decay or penetration, and accompanied by an accidental in-time γ.

A scatter plot of the mass of the 43 survivors vs $p_0'^2$ demonstrates that we observed no candidates within ± 10 MeV of m_K, and that the predominant background is $K_{\pi 3}^0$ decays.

The Monte Carlo generation of the decay $K_L^0 \to \mu\mu\gamma$ employed the matrix elements given by Sehgal.[42] The rate for the process depends on a knowledge of the $K_L^0 \to \gamma\gamma$ vertex when one of the photons is off the mass shell. The dependence of this vertex on t, the invariant (mass)^2 of the virtual photon, is expressed using a form factor
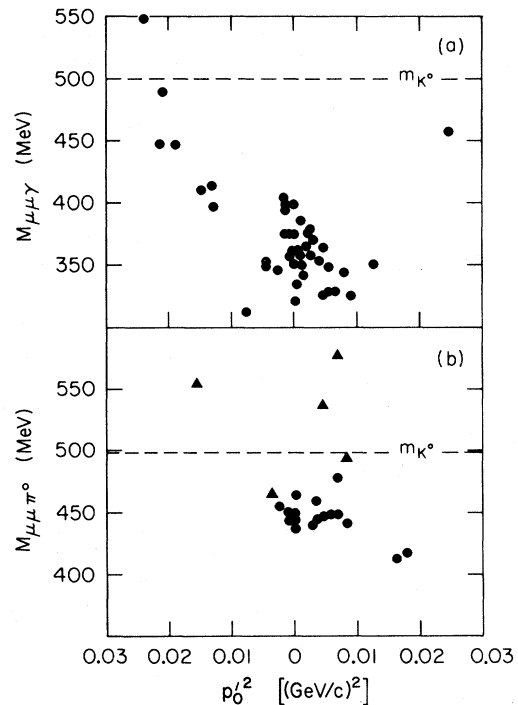

FIG. 12. Reconstructed mass of (a) $K_L^0 \to \mu^+\mu^-\gamma$, (b) $K_L^0 \to \mu^+\mu^-\pi^0$ events versus $p_0'^2$. Events plotted as triangles in (b) have $m_{2\gamma} > 500$ MeV/c^2.

$F_2(t)$. In the limit when F_2 is constant, the differential decay rate for the Dalitz process is given by

$$\frac{d\Gamma(K_L^0 \to l\bar{l}\gamma)/dt}{\Gamma(K_L \to \gamma\gamma)} = \frac{2\alpha}{\pi}\left(1 - \frac{t}{m_K^2}\right)^3\left(1 + \frac{2m_l^2}{t}\right)$$

$$\times \left(1 - \frac{4m_l^2}{t}\right)^{1/2}\frac{1}{t} ,$$

where m_K and m_l are the kaon and lepton masses. If F_2 is not constant, a significant deviation from the above may result. Sehgal displays this displacement graphically, and we employed a matrix element with a vector-meson form factor included.

We have observed no events conforming to the hypothesis $K_L^0 \to \mu\mu\gamma$. Based on the Monte Carlo acceptance of 9.26×10^{-3}, this yields a branching ratio $\Gamma(K_L^0 \to \mu^+\mu^-\gamma)/\Gamma(K_L^0 \to \pi^+\pi^-\pi^0) < 6.20 \times 10^{-5}$ at the 90% confidence level. Using $\Gamma(K_L^0 \to \pi^+\pi^-\pi^0)/\Gamma(K_L^0 \to \text{all}) = 0.126$, we obtain

$$\Gamma(K_L^0 \to \mu^+\mu^-\gamma)/\Gamma(K_L^0 \to \text{all}) < 7.81 \times 10^{-6} \ (90\% \text{CL}) .$$

This upper limit excludes the Alles and Pati model.[44] In addition, a recent Russian experiment[48] has shown that $\Gamma(K_L^0 \to e^+e^-\gamma)/\Gamma(K_L^0 \to \text{all}) < 2.8 \times 10^{-5}$ which is about a factor of 50 lower than the Alles-Pati prediction. Unfortunately the more interesting predictions, and even the Dalitz-pair rate, are more than an order of magnitude below these limits.

b. $K_L^0 \to \mu^+\mu^-\pi^0$. Both one- and two-shower events were tested as $K_L^0 \to \mu^+\mu^-\pi^0$ candidates, and the following kinematical requirements were imposed:

(1) $m_{\mu\mu} < m_K - m_{\pi^0}$,

(2) $p_{\pi^0}^* > 0$, where $p_{\pi^0}^*$ is the momentum of the π^0 in the K_L^0 rest system, and

(3) $p_{\pi^0}^T < p_{\pi^0}^*$, where $p_{\pi^0}^T$ is the transverse momentum of the π^0 in the laboratory.

These reduced 427 $\mu^+\mu^-\pi^0$ candidates to 333, of which 35 had two showers. There were sufficient constraints to determine the direction of the π^0, which must lie in the plane containing the two γ's, and also in the plane containing the direction of the K_L^0 and the transverse momentum of the charged pair. The π^0 direction together with the opening angle of the 2γ system allowed a computation of $m_{\mu\mu\pi^0}$. A scatter plot of $m_{\mu\mu\pi^0}$ versus $p_0'^2$ is shown in Fig. 12(b). No requirements whatsoever have been made on the reconstructed mass of the 2γ system, in order to display the origin of the remaining background. The events plotted as triangles have the $\gamma\gamma$ mass (which should equal m_{π^0}) greater than 500 MeV. Eliminating these events changed the acceptance by less than 2%. Virtually all the background had positive $p_0'^2$ and were therefore primarily due to $K_{\pi3}^0$ decays.

The Monte Carlo acceptance was calculated using a pure phase-space distribution, for which the

overall acceptance was 1.27×10^{-3}. At the 90% confidence level, we find that

$$\Gamma(K_L^0 \to \mu\mu\pi^0)/\Gamma(K_L^0 \to \text{all}) \leq 5.66 \times 10^{-5} ,$$

where again the normalization to $K_{\pi3}^0$ is implied. This value is consistent with the prediction of Okubo and Bace.

V. THE DECAY $K_L^0 \to \pi^+\pi^-e^+e^-$

A. Theory

The four-body decays of the K_L^0 are poorly understood, both from the theoretical point of view and experimentally because of the degree of difficulty involved. At this time, only a few four-body branching ratios have been published for the neutral kaon: a Russian streamer-chamber result for $K_L^0 \to \pi\pi ee$ (see Ref. 49) and a CERN bubble-chamber result for $K_L^0 \to \pi e\nu\gamma$.[50] Again, the predictions and the experimental values are displayed in Table III.

Experimentally, the decay $K_L^0 \to \pi\pi ee$ will be highly constrained, since the probability of an accidental vertex involving four charged tracks is very low. In this case, the process wherein the lepton pair originates in a Dalitz pair from the decay $K_L^0 \to \pi\pi\gamma$ decay is very rare, since the $\pi\pi\gamma$ rate itself is of order 10^{-5}. Thus the $\pi\pi ee$ decay is expected to be dominated by a pole graph[50] as shown in Fig. 13. Such a transition is sensitive to the electromagnetic form factor of the K_L^0, which in turn provides information about the charge radius or size of the K_L^0 through the relation $F_{K^0}(t) \approx \frac{1}{6}tR_K^2$, where $R_K^2 = $ mean squared charged distribution radius, and $F_{K^0}(t) = $ electromagnetic form factor of K_L^0.[51]

B. Kinematical analysis

The decay $K_L^0 \to \pi^+\pi^-e^+e^-$ requires a somewhat different treatment from the other decays in that four charged tracks originate at the decay vertex. Experimentally, the data sample is very clean and the principal backgrounds were expected to be $K_{\pi3}^0$ decays with the π^0 undergoing a subsequent
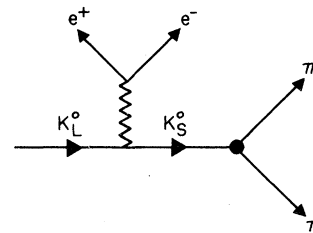

FIG. 13. Pole graph for $K_L^0 \to \pi^+\pi^-e^+e^-$ via a $K_L^0 \to K_S^0\gamma$ transition.

Dalitz decay $\pi^0 \to e^+e^-\gamma$, or an interaction of the beam with the material in the spectrometer.

To start with, we accepted only four-prong vertexes for which sufficient constraints were available even if one of these prongs did not pass through the analyzing magnet. Two data samples were generated: one having all four segments matched through the magnet to make four tracks ($4T$), the other having three full tracks with an extra front track segment ($3T + F$). As in the other decays, stringent requirements were made on the quality of the vertex and the match between the front and rear track segments. The following several additional requirements were imposed on the data: (1) The event must satisfy a $2T \cdot 3A$ trigger; (2) it must possess the proper charge combination ($+ + - -$ for $4T$, $+ + -$ or $- - +$ for $3T + F$); (3) no track may be identified as a muon; (4) the opening angle between each oppositely charged pair must be such that $\cos\theta_\pm < 0.9999$; (5) the separations in X and Y must be greater than 0.5 cm at the first plane of the wire chambers. Cuts (1), (4), and (5) eliminated a large fraction of the candidates which could not be duplicated by the Monte Carlo simulation. The charge combination cut passed both signal and $K_{\pi 3}^0$ background, but rejected a subset of accidental vertices.

The kinematic reconstruction depended primarily on the conservation of momentum. Thus we did not make assumptions about the masses of the particles and electron identification was unnecessary. For both $4T$ and $3T + F$ candidates, we required that the back-to-back angle in the transverse plane be consistent with transverse momentum balance. Each full track has an associated momentum and we defined

$$\vec{p}_{123} = \sum_{i=1}^{3} \vec{p}_i \, .$$

We denote the component of this momentum in the plane perpendicular to the K_L^0 ad $\vec{p}_{123}^T$. Then with

$$\cos\theta_{123,4} = \vec{p}_{123}^T \cdot \vec{p}_4^T \, ,$$

we demanded that $(1 + \cos\theta_{123,4}) < 0.025$. Furthermore, we computed $p_0'^2$ for all pairs of $(+, -)$ tracks and took the value closest to zero, assigning pion masses to that particular $(+ -)$ pair. We required $p_0'^2 > -0.020$ for the chosen pair, thereby reducing potential contamination due to leptonic decays and beam interactions.

At this point, the analysis for $4T$ and $3T + F$ data diverged. The background for the $3T + F$ candidates was somewhat harder to understand, and consequently we prefer to regard the $3T + F$ data as a consistency check for the $4T$ sample. After the aforementioned cuts, the 672 original

$4T$ candidates were reduced to 10. We constructed $\vec{p}_{1234}$ and the corresponding direction $\hat{\epsilon}_{1234}$,

$$\vec{p}_{1234} = \sum_{i=1}^{4} \vec{p}_i \text{ and } \hat{\epsilon}_{1234} = \frac{\vec{p}_{1234}}{|\vec{p}_{1234}|} \, .$$

For the $\pi\pi ee$ signal, $\hat{\epsilon}_K$ and $\hat{\epsilon}_{1234}$ must be colinear:

$$\cos\theta_{1234,K} = \hat{\epsilon}_K \cdot \hat{\epsilon}_{1234} \approx 1 \, .$$

We found that 20 candidates scattered widely on the $\cos\theta_{1234,K}$ plot, with no events remaining in the region $1.0 - \cos\theta_{1234,K} < 2.5 \times 10^{-6}$ which would have contained $> 99\%$ of the Monte Carlo data surviving similar cuts.

To conform our understanding of the origin of the candidates, we generated a sample of $K_L^0 \to \pi^+\pi^-\pi^0$ events wherein the π^0 underwent a subsequent Dalitz decay. This technique took into account the variation of the Dalitz-pair matrix element[52] over five orders of magnitude and the sensitivity of the resulting acceptance. We found nine Monte Carlo events surviving the cuts made on the data, with 2.3 events having $\cos\theta_{1234,K} < 2.5 \times 10^{-6}$, as opposed to 10 and 0 events respectively in the data. We conclude that the contamination from $K_{\pi 3}^0$ decays alone is sufficient to account for the observed candidates, and the distributions appear to be reasonably reproduced.

In addition we have consistency check on the $4T$ data using the $3T + F$ events, for which there were originally 4073 candidates. We imposed the same restrictions as for $4T$ candidates, with the additional demand that the missing segment would not have been observed after the magnet if the decay were actually $K_L^0 \to \pi\pi ee$. The momentum of the fourth track was computed by balancing the transverse momentum,

$$|\vec{p}_4| = \frac{|\vec{p}_{123}|}{\sin\theta_{4K}} \, ,$$

where θ_{4K} is the angle between the fourth prong and the kaon. For the data, we observed six candidates after the above cuts, and from the $K_{\pi 3}^0$ simulation, we expected 4.8. (Without the "back-to-back" cut on $\cos\theta_{123,4}$, we would have had 20 candidates, 17 from $K_{\pi 3}^0$ decays.) Although the statistics are poor, we believe that we would have detected real $K_L^0 \to \pi\pi ee$ events if they were present, and also that we understand the behavior of the background.

We estimated the acceptance by generating $K_L^0 \to \pi\pi ee$ decays using a phase-space distribution only, and this together with the observed distributions allowed us to compute the upper limit for this process. Based on the $4T$ sample, for which the final acceptance was 8.2×10^{-3}, we find that

$$\Gamma(K_L^0 \to \pi^+\pi^-e^+e^-)/\Gamma(K_L^0 \to \text{all}) \leq 8.81 \times 10^{-6}$$

at the 90% confidence level. The corresponding upper limit from the $(3T+F)$ sample is $\sim 2 \times 10^{-5}$.

Our upper limit is a slight improvement over the current experimental value of 3×10^{-5}; however, it is well above the rate expected from γ conversion in the decay $K_L^0 \rightarrow \pi\pi\gamma$ as well as the theoretical predictions.[47,53]

VI. THE DECAY $K_L^0 \rightarrow \pi^0\pi^{\pm}e^{\mp}\nu$

A. Theory

The decay $K_L^0 \rightarrow \pi^0\pi^{\pm}e^{\mp}\nu$ is the neutral analog of the charged $K_{e4}^{\pm}$ decays. One of the interesting features of this decay is its potential to differentiate among several parametrizations of $K_{e4}^{\pm}$ form factors.[54] Several experiments[55-57] on charged $K_{e4}^{\pm}$ decays have not been able to resolve which of the several schemes[58-60] is favored by the data. Experimentally, this decay presents considerable difficulties due to its kinematic similarity to $K_L^0 \rightarrow \pi^+\pi^-\pi^0$ which will constitute a large background. The final state $\pi^0\pi^{\pm}e^{\mp}\nu$ is an extremely difficult channel to reconstruct, since the neutrino is not detected and the presence of a π^0 must be inferred by observing its decay into photons.

B. Kinematical analysis

We begin by selecting events in which the two charged tracks have been identified as a pion and an electron and required two γ showers. The π^0 direction must lie between the γ's, and since the π^0 decay distribution is isotropic in its center of mass, its direction will tend to bisect the 2γ opening angle in the laboratory system. We therefore assumed this to be the π^0 direction.

In contrast to the other decay modes, we relied on the timing information directly to establish the K_L^0 momentum. This was necessary, but unaesthetic for several reasons. First, the momentum resolution was related to the timing error by $\Delta p/p = \gamma^2 \Delta T/T$, where $\gamma = E_K/m_K$. Second, the timing resolution was not easily duplicated in the Monte Carlo simulation and to this extent the Monte Carlo acceptance did not reflect the processes in the spectrometer.

The following kinematical requirements were imposed on the decay:

(1) $p_0'^2 < -0.005$ to reduce $K_{\pi 3}^0$ contamination,

(2) $m_{\pi e} < m_K - m_{\pi^0}$ to reduce K_{l3}^0 contamination,

(3) $\cos\theta_{\gamma e} < 0.9996$ to reduce bremsstrahlung photons, $\cos\theta_{\gamma\pi} < 0.9999$,

(4) the p_{π^0} requirements

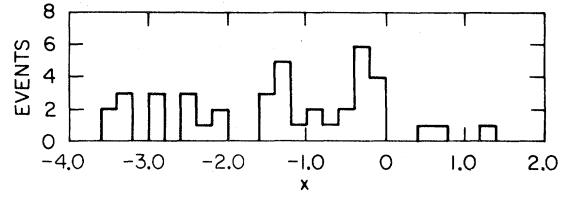(a) $p_{\pi^0}/p_K < 0.6$,

(b) $p_{\pi^0} < 6$ GeV/c,

FIG. 14. Reconstructed neutrino mass^2 in $K_L^0 \rightarrow \pi^0\pi e\nu$ decay, $x = m_\nu^2/m_{\pi^0}^2$.

(c) $y^2 < 2$, where

$$y^2 \equiv p_{\pi^0}^2/(p_K^2 + p_{\pi e}^2 - 2\vec{p}_K \cdot \vec{p}_{\pi e})$$

$$= 1 + \frac{(p_\nu^2 - 2\vec{p}_K \cdot \vec{p}_\nu + 2\vec{p}_{\pi e} \cdot \vec{p}_\nu)}{(p_K^2 + p_{\pi e}^2 - 2\vec{p}_K \cdot \vec{p}_{\pi e})}.$$

The acceptance for $\pi^0\pi e\nu$ events was very small, since the $p_0'^2$ cut passed only 43% of the data, and the photon conversion further reduced the sample by a factor of 4. The variable $x \equiv m_\nu^2/m_{\pi^0}^2$ is plotted in Fig. 14, where there are 17 events with $|x| \leq 1.0$, where we expect to find 64% of the signal.

We expect the following several background processes to contribute: (1) $K_{\pi 3}^0$ decays in which a pion has been misidentified as an electron, with the two showers arising from a combination of real or accidental photons; (2) K_{e3}^0 decays having two spurious showers. These sources were simulated by a Monte Carlo simulation, and we estimate the expected number of accidental events to be 9 ± 3.3, where systematic effects have been included. We subtract the expected background from the observed distribution to obtain the final number of candidates:

$$N(\pi^0\pi e\nu) = 17 \pm \sqrt{17} - (9 \pm 3.3) = 8 \pm 5.2.$$

Using the Monte Carlo generated acceptance of 2.88×10^{-4}, we find the corresponding limit on the branching ratio to be

$$\Gamma(K_L^0 \rightarrow \pi^0\pi^{\pm}e^{\mp}\nu)/\Gamma(K_L^0 \rightarrow \text{all}) \leq 2.2 \times 10^{-3} \text{ at 90\% CL}.$$

Owing to the extreme contortions necessary to eliminate backgrounds in this channel, the remaining sensitivity is quite insufficient to attain even the relatively modest levels needed to discriminate between the various models and the current-algebra calculation shown in Table III.

*Work supported in part by the Energy Research and Development Administration.

†Present address: Brookhaven National Laboratory, Upton, N.Y. 11973.

‡Present address: Rockefeller University, New York, N.Y. 10021.

[1]R. Piccioni, SLAC Report No. SLAC-155, (unpublished).

[2]R. Messner, University of Colorado, thesis, 1974 (unpublished).

[3]R. Piccioni, G. Donaldson, D. Fryberger, D. Hitlin, J. Liu, B. Meyer, A. Rothenberg, M. Schwartz, D. Uggla, and S. Wojcicki, Phys. Rev. D 9, 2939 (1974).

[4]R. Coombes, D. Fryberger, D. Hitlin, R. Piccioni, and D. Porat, Nucl. Instrum. Methods 98, 317 (1972).

[5]G. Donaldson, D. Fryberger, D. Hitlin, J. Liu, B. Meyer, R. Piccioni, A. Rothenberg, D. Uggla, S. Wojcicki, and D. Dorfan, Phys. Rev. D 9, 2960 (1974).

[6]B. Rossi, *High Energy Particles* (Prentice-Hall, Englewood Cliffs, New Jersey, 1952).

[7]D. Sober, R. Haddock, B. Nefkens, and B. Schrock, Nucl. Instrum. Methods 109, 29 (1973).

[8]R. Messner, A. Franklin, R. Morse, U. Nauenberg, D. Hitlin, J. Liu, R. Piccioni, and D. Dorfan, Phys. Rev. Lett. 33, 1458 (1974).

[9]J. Bernstein, G. Feinberg, and T. D. Lee, Phys. Rev. 139, B1650 (1965).

[10]R. Abrams, A. Carroll, T. Kycia, K. Li, J. Menes, D. Michael, P. Mockett, and R. Rubinstein, Phys. Rev. Lett. 29, 1118 (1972).

[11]R. Abrams, A. Carvell, T. Kycia, K. Li, J. Menes, D. Michael, P. Mockett, and R. Rubinstein, Phys. Rev. Lett. 30, 500 (1973).

[12]G. Bergun, P. Bertranet, E. Lesquoy, A. Muller, E. Pauli, S. Zylberajch, F. James, L. Montanet, E. Paul, S. Saetre, and D. Sendall, Phys. Lett. 46B, 481 (1973).

[13]A. Dolgov and L. Ponomarev, Yad. Fiz. 4, 367 (1966) [Sov. J. Nucl. Phys. 4, 262 (1967)].

[14]G. Costa and P. Kabir, Nuovo Cimento 51A, 564 (1967).

[15]L. Sehgal and L. Wolfenstein, Phys. Rev. 162, 1362 (1967).

[16]D. Beder, Nucl. Phys. B47, 286 (1972).

[17]C. S. Lai and B. L. Young, Nuovo Cimento 52A, 83 (1967).

[18]H. Chew, Nuovo Cimento 26, 1109 (1962).

[19]S. V. Pepper and Y. Ueda, Nuovo Cimento 33, 1461 (1964).

[20]S. Oneda, Y. S. Kim, and D. Korff, Phys. Rev. 136, B1064 (1964).

[21]D. Cline, Nuovo Cimento 36, 1055 (1965).

[22]R. C. Thatcher, University of Illinois, thesis, COO-1195-113 (unpublished). See also Ref. 5.

[23]All branching ratios quoted herein are from Rev. Mod. Phys. 45, No. 2, Part II, S1–S175 (1973).

[24]R. Rockmore, Phys. Rev. D 1, 226 (1970).

[25]S. Barshay, Phys. Lett. 36B, 571 (1971).

[26]M. Moshe and P. Singer, Phys. Rev. D 6, 1379 (1972).

[27]M. Moshe and P. Singer, Tel Aviv Report No. PRINT 74-1257, 1974 (unpublished).

[28]P. Singer, in *Proceedings of the European Physical Society International Conference on Meson Resonances and Related Electromagnetic Phenomena, Bologna, Italy, 1971,* edited by R. H. Dalitz and A. Zichichi (Editrice Compositori, Bologna, Italy, 1972).

[29]A. Browman, J. DeWire, B. Gittelman, K. Hanson,

E. Loh, and R. Lewis, Phys. Rev. Lett. 32, 1067 (1974).

[30]J. Steinberger, Phys. Rev. 76, 1180 (1949).

[31]R. Rockmore and T. Wong, Phys. Rev. Lett. 28, 1736 (1972).

[32]R. Rockmore and T. F. Wong, Phys. Rev. D 7, 3425 (1973).

[33]A. Clark, T. Elioff, R. Field, H. Frisch, R. Johnson, L. Kerth, and W. Menzel, Phys. Rev. Lett. 26, 1667 (1971).

[34]H. Stern and M. Gaillard, Ann. Phys. (N.Y.) 76, 580 (1973).

[35]R. C. Thatcher, A. Abashian, R. J. Abrams, D. W. Carpenter, R. E. Mishke, B. M. K. Nefkens, J. H. Smith, L. J. Verhey, and A. Wattenberg, Phys. Rev. 174, 1674 (1968).

[36]B. M. K. Nefkens, A. Abashian, R. J. Abrams, D. W. Carpenter, G. P. Fisher, and J. H. Smith, Phys. Lett. 19, 706 (1966).

[37]E. Bellotti, A. Pullia, M. Baldo-Ceolin, E. Calimani, S. Ciampolillo, H. Huzita, F. Mattioli, and A. Sconza, Nuovo Cimento 45, 737 (1966).

[38]M. Anikina, G. Vardenga, M. Zhuravleva, D. Kotlyarevskii, D. Neagu, E. Okonov, G. Takhtamyshev, Wu Tsung-fan, and L. Chkhaidze, Yad. Fiz. 2, 853 (1965) [Sov. J. Nucl. Phys. 2, 609 (1966)].

[39]B. Martin, E. de Rafael, and J. Smith, Phys. Rev. D 2, 179 (1970).

[40]W. Alles, M. Gaillard, J. Pati, Phys. Rev. D 8, 2299 (1973).

[41]T. Miyazaki, Lett. Nuovo Cimento 3, 293 (1972).

[42]L. Sehgal, Phys. Rev. D 7, 3303 (1973).

[43]S. Singh, Phys. Rev. D 6, 2646 (1972).

[44]W. Alles and J. Pati, Nuovo Cimento 10A, 325 (1972).

[45]A. Pais and S. Treiman, Phys. Rev. 176, 1974 (1968).

[46]S. Singh and L. Wolfenstein, Nucl. Phys. B24, 77 (1972).

[47]S. Okubo and M. Bace, Nucl. Phys. B40, 541 (1970).

[48]V. V. Barmin, G. Davidenko, V. Demidov, A. Dolgolenko, V. Matveev, A. Meshkovskii, G. Mirosidi, T. Christyakova, I. Chuvilo, and V. Shebanov, Yad. Fiz. 15, 1149 (1972) [Sov. J. Nucl. Phys. 15, 636 (1972)].

[49]M. Anikina, V. Balashov, B. Bannik, H. Vardenga, M. Zhuravljiova, V. Iljina, J. Lukstinsh, E. Matlsev, V. Moros, E. Okonov, T. Ostanevich, G. Ttentjukova, J. Cherepoanov, and S. Khorozov, Report No. PRINT 72-3826, Dubna, 1972 (unpublished).

[50]G. Evans, J. Muir, K. Peach, I. Budagov, H. Hopkins, W. Krenz, F. Nezrick, and R. Worthington, Phys. Lett. 35B, 351 (1971).

[51]L. Kondratyuk, L. Panomarev, and V. Zakharov, Phys. Lett. 27B, 655 (1968).

[52]D. Joseph, Nuovo Cimento 16, 997 (1960).

[53]D. Majumdar and J. Smith, Phys. Rev. 187, 2039 (1969).

[54]A. Pais and S. Treiman, Phys. Rev. 168, 1858 (1968).

[55]P. Basile, S. Brehin, A. Diamant-Berger, P. Kunz, M. Lemoine, R. Turlay, A. Zylbersztejn, M. Bourquin, J. Boymund, P. Exterman, J. Marasco, R. Mermod, P. Piroue, and H. Suter, Phys. Lett. 36B, 619 (1971).

[56]R. Ely, G. Gidal, V. Hagopian, G. Kalmus, K. Billings, F. Bullock, M. Esten, M. Govan, C. Henderson, W. Knight, F. Stannard, O. Treutler, U. Camarini, D. Cline, W. Fry, H. Haggarty, R. March, and W. Singleton, Phys. Rev. 180, 1319 (1969).

[57]W. Schweinberger, D. Bertrand, M. Czejthey-Barth, P. Van Binst, W. Knight, J. Lemonne, C. Esueld, F. Bobisut, M. Mattioli, and G. Miari, Phys. Lett. <u>36B</u>, 246 (1971).

[58]F. Berends, A. Donnachie, and G. Oades, Phys. Lett. <u>26B</u>, 109 (1967).

[59]M. Bace and S. Okubo, Phys. Lett. <u>38B</u>, 429 (1972).

[60]S. Weinberg, Phys. Rev. Lett. <u>17</u>, 336 (1966).